ARTICLE
Journal of Cellular Biochemistry 116:2667–2675 (2015)

Journal of Cellular Biochemistry

In situ Analysis of Smoothelin-like 1 and Calmodulin Interactions in Smooth Muscle Cells by Proximity Ligation

Annegret Ulke-Lemée, Sara R. Turner, and Justin A. MacDonald*

Department of Biochemistry and Molecular Biology, Cumming School of Medicine, University of Calgary, Calgary, Alberta T2N 4Z6, Canada

ABSTRACT

The smoothelin-like 1 (SMTNL1) protein is the newest member of the smoothelin family of muscle proteins. Two calmodulin (CaM)-binding domains (CBD1 for Ca-CaM; CBD2 for apo-CaM) have been described for the SMTNL1 protein using in vitro assays. We now demonstrate in situ associations of SMTNL1 and CaM in A7r5 smooth muscle cells using the proximity ligation assay (PLA). We quantified CaM-SMTNL1 proximity events accurately after taking into account variations in protein expression levels. The refined method allows quantification of in situ proximity after transient transfection with an associated error of $<10\%$. The proximity of SMTNL1 and CaM in A7r5 cells could be reduced by scrambling the amino acid sequence and mutation of large hydrophobic amino acids of CBD1. The truncation of CBD2 did not influence SMTNL1 proximity to CaM. Ultimately, we conclude that SMTNL1 forms complex interactions with CaM in smooth muscle cells, with a role for CBD1 and possibly the intrinsically disordered region. J. Cell. Biochem. 116: 2667–2675, 2015.

KEY WORDS: CHASM; SMTNL1; CALPONIN HOMOLOGY DOMAIN; CALMODULIN-BINDING DOMAIN

INTRODUCTION

Smoothelin-like 1 protein (SMTNL1, also known as the calponin homology-associated with smooth muscle protein, CHASM) belongs to the smoothelin family of muscle proteins [Borman et al., 2004; Turner and MacDonald, 2014]. SMTNL1 was originally identified as a modulator of smooth muscle calcium sensitization, and additional findings have revealed the protein to play a role in cardiovascular and skeletal muscle adaptations to exercise [Wooldridge et al., 2008], autoregulatory constrictions of the microvasculature in response to changes in transmural pressure and circumferential wall-stress [Turner and MacDonald, 2014], as well as transcriptional programming of smooth muscle during pregnancy [Lontay et al., 2010; Bodoor et al., 2011].

The smoothelins are specifically expressed in, and frequently used as markers of, differentiated contractile smooth muscle cells [van der Loop et al., 1996]. Two isoforms of smoothelin have been identified: a 59 kDa isoform (smoothelin-A) that is expressed in visceral smooth muscle such as intestine [Kramer et al., 1999; Niessen et al., 2005], and a 100 kDa isoform (smoothelin-B) that is expressed in vascular smooth muscle [Wehrens et al., 1997; Kramer et al., 2001]. Knowledge pertaining to their physiological functions remains limited; however, the smoothelin members are hypothesized to belong to a smooth muscle tropomyosin-troponin-like system [Quensel et al., 2002]. It appears that smoothelins may lock smooth muscle cells in a contractile phenotype, possibly by stabilizing key structural proteins comprising the actin thin-filament [Niessen et al., 2004].

The C-terminus of SMTNL1 contains a calponin homology (CH)-domain (residues 342–459) that is also found in the other smoothelin proteins, whereas the N-terminal domain (residues 1–341) is composed of unique sequence that forms an intrinsically disordered region (IDR). Notably, CH-domains are found in a variety of cytoskeletal and signaling proteins that play regulatory roles in cellular contraction [Gimona et al., 2002]. We have discovered that the CH-domain in combination with a portion of the IDR can direct SMTNL1 binding to tropomyosin and likely contributes to the localization of SMTNL1 with the thin filament [Ulke-Lemee et al., 2010; MacDonald et al., 2012]. Moreover, we have also identified that SMTNL1 can bind apo-calmodulin (apo-CaM) and Ca^{2+}-associated CaM (Ca-CaM) through two unique CaM-binding domains (CBDs). One CBD is located within the CH-domain and binds apo-CaM through an IQ-motif (CBD2: [Ishida et al., 2008]), and the other is located within the IDR just upstream of the CH-domain

Grant sponsor: Canadian Institutes of Health Research (CIHR); Grant number: MOP-97931.

*Correspondence to: Justin A. MacDonald, Smooth Muscle Research Group at the Libin Cardiovascular Institute of Alberta, Cumming School of Medicine, 3280 Hospital Drive NW, Calgary, Alberta, Canada, T2N 4Z6.
E-mail: jmacdo@ucalgary.ca

Manuscript Received: 20 March 2015; Manuscript Accepted: 22 April 2015
Accepted manuscript online in Wiley Online Library (wileyonlinelibrary.com): 29 April 2015
DOI 10.1002/jcb.25215 • © 2015 Wiley Periodicals, Inc.

and confers binding to Ca-CaM and weaker binding to apo-CaM in vitro (CBD1: [Ulke-Lemee et al., 2014]).

The intracellular localization of SMTNL1 may be conferred by association with tropomyosin at the thin filament, an event that has been hypothesized to be influenced by CaM-binding since the CBD1 is located in the vicinity of the tropomyosin-binding domain and could act as an effector domain [Ulke-Lemee et al., 2010; MacDonald et al., 2012]. The CaM-binding properties of CBD1 and CBD2 have been described for SMTNL1 using a variety of in vitro biophysical techniques; however, data that demonstrate in situ associations of SMTNL1 and CaM are still lacking. In this study, we used confocal microscopy and the proximal ligation assay (PLA) to investigate the association of SMTNL1 and CaM within rat aortic (A7r5) smooth muscle cells. In order to quantify changes in PLA events for CaM with different SMTNL1 mutants, we developed and validated a PLA method that corrects for variations in target protein expression. The investigations suggest that CBD1 of SMTNL1 contributes to proximity to CaM within A7r5 smooth muscle cells, whereas CBD2 does not play a role.

MATERIALS AND METHODS

MATERIALS

Anti-calmodulin (rabbit monoclonal EP799Y, ab45689) and anti-smooth muscle α-actin (rabbit polyclonal, ab125044) antibodies were from Abcam Inc. (Toronto, ON). Anti-FLAG M2 (mouse monoclonal, F1804) and anti-FLAG (rabbit monoclonal, F7425) antibodies were from Sigma Chemical Co. (St. Louis, MO). Rabbit anti-GFP (sc-8334) antibody was from Santa-Cruz (Dallas, TX) and AlexaFluor568-goat anti-mouse antibody (A-11004) was from Life Technologies (Burlington, ON). The Duolink In situ Proximity Ligation Assay kit was purchased from Olink Bioscience (Uppsala, Sweden). All other chemicals were of reagent grade and were obtained from VWR (Edmonton, AB) or Sigma Chemical Co.

CLONING OF EXPRESSION CONSTRUCTS

Murine *Smtnl1* (GenBank ID: EDL27304.1) was cloned into Xho1 and EcoR1 restriction sites of the bicistronic pIRES-AcGFP1 vector (Clontech, Mountain View, CA) with a 5′-FLAG-tag (DYKDDDDK) using standard cloning techniques. The resulting pIRES-AcGFP1-FLAG-SMTNL1 vector has an internal ribosome entry site that permits the co-expression of *Aequorea coerulescens* green fluorescent protein (AcGFP) with FLAG-SMTNL1. We also generated the following SMTNL1 clones in the pIRES-AcGFP1-FLAG background (see also Supplementary Figure S1 and [Ulke-Lemee et al., 2014]): SMTNL1 with a scrambled CBD1 sequence (scrCBD1), SMTNL1 with deletion of the CBD1 sequence (ΔCBD1), SMTNL1 with truncation of CBD2's C-terminal ^{455}KTKKK^{459} sequence (Δ4K), and SMTNL1 with alterations in both CBD sequences (scrCBD1-Δ4K and ΔCBD1-Δ4K). A pcDNA3.1-FLAG-NCKX2 construct expressing the human sodium-potassium-calcium exchanger 2 was a kind gift from Dr. Jonathan Lytton (University of Calgary).

CELL CULTURE AND TRANSFECTION

Rat thoracic aorta smooth muscle cells (A7r5, CRL-1444, ATCC, Manassas, VA) were maintained in Dulbecco's-modified Eagle Medium (DMEM, Life Technologies) supplemented with 10% (v/v) heat-inactivated fetal bovine serum (FBS). Cells were plated on fibronectin-coated glass coverslips (Fisher Scientific, Ottawa, ON), grown to 70% confluency and transfected using Lipofectamine LTX or Lipofectamine 2000 (Life Technologies) following the manufacturer's protocols. Cells were used 24 h after transfection for immunocytochemistry, PLA or western blotting.

WESTERN BLOTTING

Wells containing transfected A7r5 cells were washed twice with PBS, and whole cell lysates were prepared by harvesting with SDS-PAGE loading buffer. Proteins were detected after transfer to 0.2 μm PVDF membrane using anti-FLAG (rabbit, F7425), anti-smooth muscle α-actin or anti-GFP antibodies using standard methods. All western blots were visualized with a LAS4000 Imaging Station (GE Healthcare) after incubation with ECL Western blotting detection reagent or SuperSignal West Femto Reagent (GE Healthcare, Piscataway, NJ).

PROXIMITY LIGATION ASSAY AND IMMUNOCYTOCHEMISTRY

Transfected A7r5 cells were washed twice in pre-warmed (37°C) PBS, fixed for 10 min in 4% (w/v) paraformaldehyde in PBS, permeabilized for 10 min with 0.3% (v/v) Triton X-100 in PBS and blocked for 1 h with 5% (v/v) normal goat serum (NGS, Life Technologies). For analysis by PLA, A7r5 cells were probed for 16 h at 4°C with anti-CaM antibody (1:200 in 5% NGS), then probed for 1 h at 22°C with anti-FLAG antibody (mouse, F1804, 1:200 in 5% NGS). After washing with PBS, the slides were developed following the manufacturer's protocol. Developed slides were mounted, stored at −20°C and imaged within 48 h. For microscopy, an Olympus FV10i confocal microscope equipped with an oil-immersion 60x objective and phase ring was used with FV10i-SW image acquisition software and Fluoview v3.0a image processing software. A7r5 cells grown and treated in parallel to the PLA experiments were processed for immunocytochemistry. After fixing as described for PLA, the slides were blocked overnight in 5% NGS, washed and then incubated for 1 h at 22°C with anti-FLAG antibody (mouse, F1804, 1:200 in 5% NGS). Following incubation with secondary AlexaFluor568 anti-mouse antibody (1:1000 in 5% NGS), slides were washed in PBS, dried and then mounted with ProLong Gold Antifade Reagent with DAPI (Life Technologies).

CALCULATIONS AND STATISTICS

All statistical calculations were performed using GraphPad / Prism (La Jolla, CA). Data are expressed as mean ± standard errors (SEM). Please refer to Supplemental Methods for a detailed overview of calculations.

RESULTS

The in situ proximity of FLAG-SMTNL1 to CaM was investigated using rat A7r5 smooth muscle cells transiently transfected with a

bicistronic vector that co-expressed FLAG-SMTNL1 together with AcGFP protein to enable the identification of those A7r5 cells that were successfully transfected. Fluorescent dots were observed for in situ PLA events when the two primary antibodies were localized in close proximity (~ 30 nm) [Soderberg et al., 2006; Koos et al., 2014]. In this case, PLA signals (i.e., red dots) were readily detected using anti-FLAG and anti-CaM antibodies together with the Duolink kit, suggesting in situ proximity of the two proteins (Fig. 1A). Of note, the PLA signals were confined to the cytosolic compartment and were excluded from the nucleus.

A panel of controls were completed to demonstrate the specificity of the PLA signal for the SMTNL1 and CaM proteins. Cells transfected with FLAG-SMTNL1 together with GFP (green) and probed with anti-FLAG and anti-CaM followed by PLA show robust PLA signal development (30–150 PLA events per cytosolic compartment, Fig. 1A). Omitting either primary antibody for CaM (Fig. 1B) or FLAG (Fig. 1C), removing the FLAG-tag from SMTNL1 (Fig. 1D) or expressing AcGFP only (Fig. 2E) all result in very few PLA signals (no CaM antibody: 1.0 ± 0.6 PLA events, Fig. 1B; no FLAG antibody: 4.7 ± 1.7 PLA events, Fig. 1C; no FLAG tag on SMTNL1 construct: 1.7 ± 0.3 PLA events, Fig. 1D; only expression of AcGFP: 0.5 ± 0.2 PLA events, Fig. 1E; all PLA events quantified in the cytosolic compartment). Replacing FLAG-SMTNL1 with the unrelated FLAG-tagged human sodium-potassium-calcium exchanger 2 (FLAG-NCKX2) showed only spurious signals with no increase in PLA events for the transfected cells (6.3 ± 1.1 PLA events per cytosolic compartment, Fig. 1F).

Significant variability in the number of PLA events for SMTNL1 and CaM was observed within individual cells among separate experiments. The variability in PLA events appeared to depend on the age of the kit, as newly opened kit reagents resulted in many PLA signals (Fig. 2A) whereas an older kit (6 months, but within the expiry date) resulted in significantly fewer PLA signals (Fig. 2B). Furthermore, the number of PLA signals found for individual A7r5 cells after transfection with FLAG-SMTNL1 varied greatly. The A7r5 cells with the most AcGFP (green) signal also exhibited the highest number of PLA signals (Fig. 2C), suggesting a correlation between the transfection efficiency and number of PLA events in any given cell.

Given the heterogeneity in PLA signals displayed by individual cells, it was not immediately possible to quantify the effects of disrupting the two distinct CBD regions on SMTNL1 and CaM proximity. So, we established whether the fluorescent AcGFP signal produced by concurrent expression with the bicistronic vector could be used to normalize the number of PLA events to the SMTNL1 protein transfection efficiency in individual cells. As a first step we verified that the AcGFP expression level was proportional to the FLAG-SMTNL1 expression level. Only those cells that possessed immunofluorescent signal from FLAG-SMTNL1 (red, Fig. 3A) displayed GFP signal (green, Fig. 3B). Again, FLAG-SMTNL1 was localized to the cytosolic compartment and excluded from the nucleus (Fig. 3C) whereas the AcGFP signal was diffusely distributed throughout. Additional cells, identified by nuclear DAPI staining and/or phase contrast, did not exhibit either fluorescent signal (Fig. 3C,D). The fluorescence signals for AcGFP and FLAG-SMTNL1 were quantified in defined regions of interest (ROI) for background and the cytosolic compartment (Fig. 3F). We calculated the "mean of the intensity" of a selected channel (AcGFP or AlexaFluor568) in all z-slices within the cytoplasmic ROI. Graphing these values for AcGFP and FLAG-SMTNL1 intensity revealed that the expression levels of the two proteins were indeed proportional ($R^2 = 0.88$, $n = 21$ cells from duplicate slides; Fig. 3G). The relationship between FLAG-SMTNL1 and AcGFP expression levels was distinct from that of FLAG-SMTNL1-Δ4K and AcGFP ($P < 0.0001$, $n = 21$; Fig. 3G), indicating that more FLAG-SMTNL1-Δ4K per AcGFP was expressed and/or detected. Western blotting showed no appreciable differences in the global expression levels of the two FLAG-SMTNL1 proteins, AcGFP and smooth muscle α-actin (Fig. 3H) among three different transfection experiments.

The quantification of PLA events was completed on transfected cells. The cytoplasmic space, excluding the nucleus as determined by DAPI-stain, was delineated by an ROI and a second ROI was drawn in the extracellular space for background subtraction (Fig. 4A). PLA signals within the ROI (i.e., red dots) were counted in all z-slices, encompassing the entire thickness of the cell (Fig. 4A–C). The "integral of the intensity" for the AcGFP fluorescence signal as well as the number of PLA events in the ROI was calculated for all z-slices (Fig. 4D). Three independent transfections of A7r5 cells gave an identical linear relationship between AcGFP intensity and the number of PLA signals (slope of 1.06 ± 0.17, $R^2 = 0.35$, $n = 68$ cells counted from three independent experiments from duplicate slides; Fig. 4E). The AcGFP signal intensity varied by a factor of ~ 15 between the lowest and the highest intensity in the cells imaged, and the PLA signal was not saturated within this range. These results establish a reproducible method that permits the quantitative assessment of in situ proximity events independent of protein expression levels.

Biochemical studies have provided evidence for two CBDs in SMTNL1 [Ishida et al., 2008; Ulke-Lemee et al., 2014], yet the relative contribution of each CBD to cellular CaM-binding in situ has not been examined. We generated SMTNL1 variants, disrupting CBD1, CBD2 or both domains (see Supplementary Figure S1) and used these FLAG-tagged SMTNL1 variants to investigate intracellular proximity with CaM in A7r5 cells. The expression of each SMTNL1 mutant provided significant numbers of PLA events (red dots), and the PLA signal abundance was strongly dependent on protein expression levels, as already noted for the wild-type FLAG-SMTNL1 protein. We quantified proximity of all FLAG-SMTNL1 mutants to CaM using the AcGFP signal for normalization of protein expression levels (Table I). The deletion of CBD1 (ΔCBD1) had no effect on SMTNL1 and CaM proximity events, whereas a scrambled CBD1-SMTNL1 (scrCBD1, retaining CBD1 amino acids in a scrambled sequence to eliminate the amphipathic helix character) showed significant reduction in proximity events. The main apo-CaM binding site of SMTNL1 is CBD2 [Ishida et al., 2008; Ulke-Lemee et al., 2014], and previous in vitro studies showed that deletion of the last five amino acids of the CBD2 (Δ4K) reduced binding. In PLA experiments, this deletion had no impact on proximity. Similarly, combining the Δ4K deletion in CBD2 with deletion of CBD1 (ΔCBD1-Δ4K) had no impact on PLA events for SMTNL1 and CaM. The final mutant tested combined the Δ4K deletion with scrambled CBD1. This mutant showed a similar reduction of proximity as for scrCBD1.

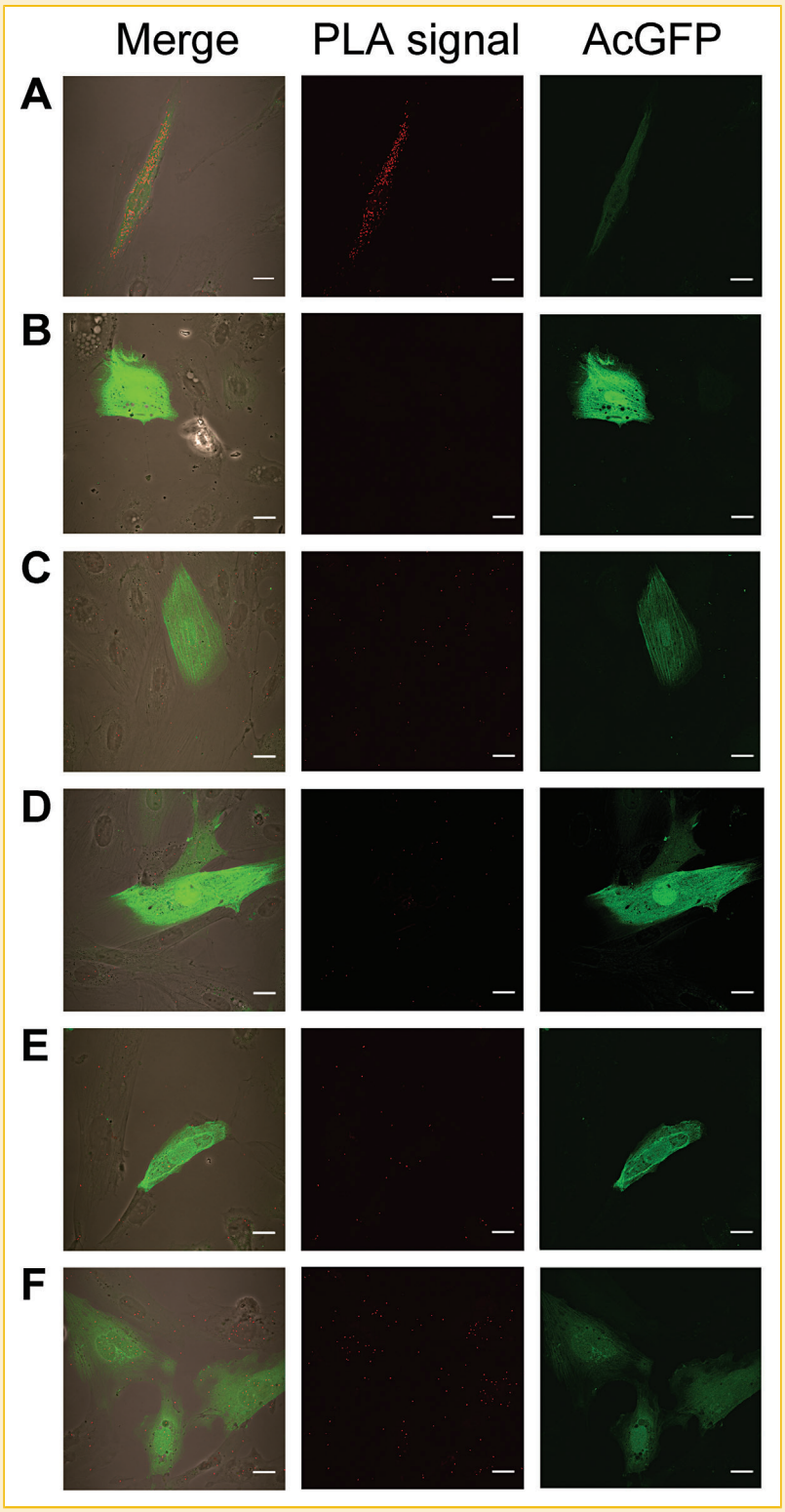

Fig. 1. PLA performed on FLAG-SMTNL1 and CaM confirms in situ proximity of proteins in A7r5 smooth muscle cells. A7r5 cells transfected with a bicistronic vector expressing various proteins together with AcGFP (green) were probed with anti-FLAG and anti-CaM antibodies using the PLA kit. The PLA signals (red dots) indicate proximity of CaM and FLAG-tagged proteins. In A, FLAG-SMTNL1 together with AcGFP was transfected and probed with both anti-FLAG and anti-CaM antibodies, followed by PLA. The anti-CaM antibody (B) or anti-FLAG (C) antibody was omitted while the transfection and PLA conditions were kept the same as in panel A. In D, the SMTNL1 protein without the FLAG-tag was transfected together with AcGFP and probed as in panel A. In E, AcGFP was transfected in the absence of FLAG-SMTNL1 and probed as in panel A. In F, FLAG-NCKX2 (human sodium-potassium-calcium exchanger 2) was expressed together with AcGFP and probed as in A. Representative images are shown with fluorescence and phase-contrast signals (Merge), PLA signals (red channel only) or AcGFP (green channel only). Scale bar: 20 μm.

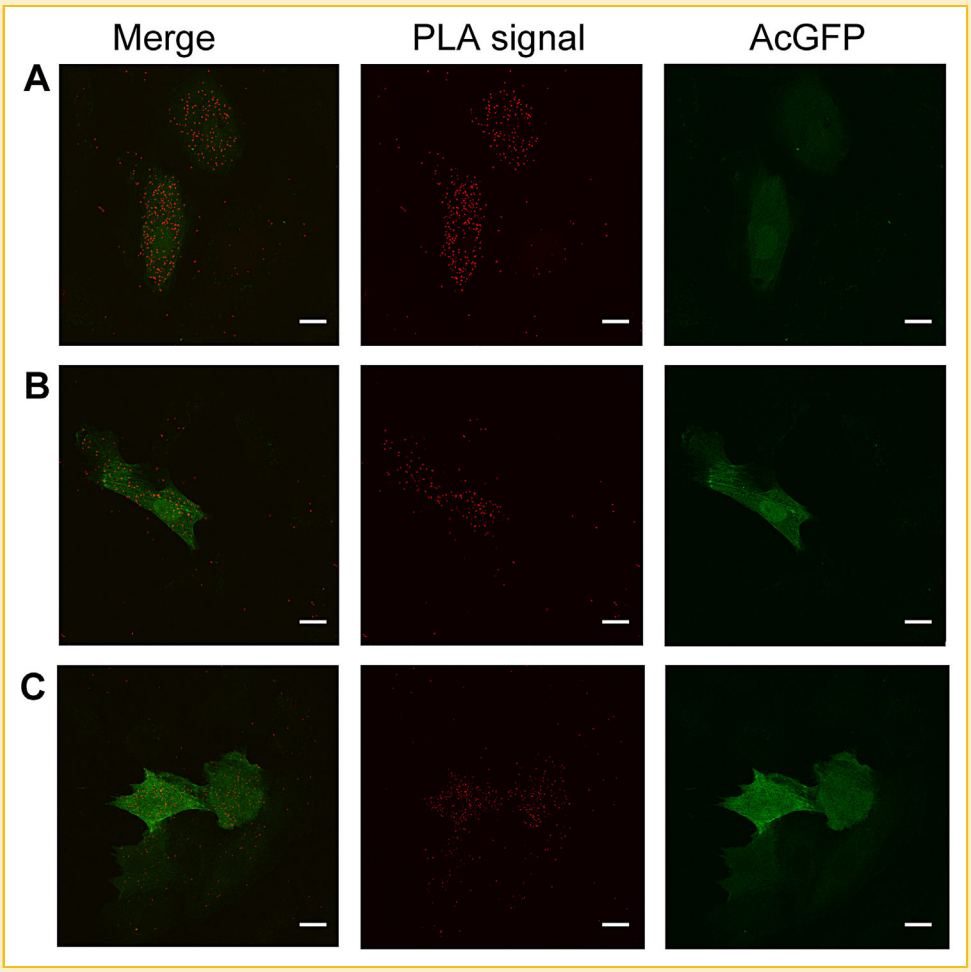

Fig. 2. PLA events vary with protein expression levels and intra-kit fluctuations. Rat A7r5 smooth muscle cells were transfected with a bicistronic vector expressing FLAG-SMTNL1 and AcGFP and probed with anti-FLAG and anti-CaM antibodies using the PLA kit. The PLA signals (red dots) indicate proximity of FLAG-SMTNL1 with CaM. FLAG-SMTNL1 expression can be deduced by the concomitant green AcGFP signal (λ_{ex} 473 nm, λ_{em} 490 ± 50 nm). A, newly-acquired PLA kit (PLA signal red, λ_{ex} 559 nm, λ_{em} 570 ± 50 nm). B, 6 months old PLA kit (PLA signal red). C, 6 month old PLA kit (PLA signal far-red; λ_{ex} 635 nm, λ_{em} 660 ± 50 nm). Representative images are shown with fluorescence and phase-contrast signals (Merge), PLA signals (red channel only) or AcGFP (green channel only). Scale bar: 20 μm.

DISCUSSION

CaM is the primary intracellular Ca^{2+} receptor, and Ca^{2+}-dependent signalling relies on the association of Ca-CaM with CBDs of target proteins (reviewed in [Chin and Means, 2000; Ishida and Vogel, 2006]). To date, hundreds of CaM-binding proteins have been described with binding affinities (K_D) of 10^{-6} - 10^{-10} M [Ikura, 2002; Ishida and Vogel, 2006; O'Connell et al., 2010]. It has also been recognized that apo-CaM can influence signalling by associating with distinct apo-CaM-binding CBDs, often containing IQ-motifs [Bahler and Rhoads, 2002]. Typically, the binding affinities for apo-CaM are much lower than those observed for Ca-CaM, with K_D values of 10^{-5}–10^{-8} M. Dozens of proteins possess CBD sequences, yet many of these CaM targets await experimental validation within the intracellular environment. Indeed, the investigation of many potentially important transient (weak) CaM complexes has likely been hindered by an inability to provide independent validation with common techniques such as co-immunoprecipitation.

The PLA method is well-suited to the investigation of interactions between CaM and its intracellular binding partners. Previously, the PLA technique was successfully applied to the examination of the calcium-dependent proximity of CaM to the immunomodulatory protein Bcl10 [Edin et al., 2010]. Herein, we apply the PLA technique to examine a specific CaM target in situ within vascular smooth muscle cells. In this case, we investigated the role of two CBDs found in SMTNL1. The proximity of endogenous CaM with transiently transfected FLAG-SMTNL1 was readily detected by PLA in unstimulated A7r5 aortic smooth muscle cells. These findings confirm our in vitro data [Ulke-Lemee et al., 2014] and establish SMTNL1 as a bona fide CaM-binding protein within smooth muscle cells.

For the investigation of protein complexes, it is often desirable to introduce proteins into cells by transient transfection. This allows investigators to employ unique epitope tags to overcome the lack of specific antibodies as well as to introduce mutations to investigate signaling after altered complex formation. While transient transfection facilitates the quick introduction of protein variants, it has the drawback that protein expression levels vary significantly between individual cells of the cell culture population. Thus,

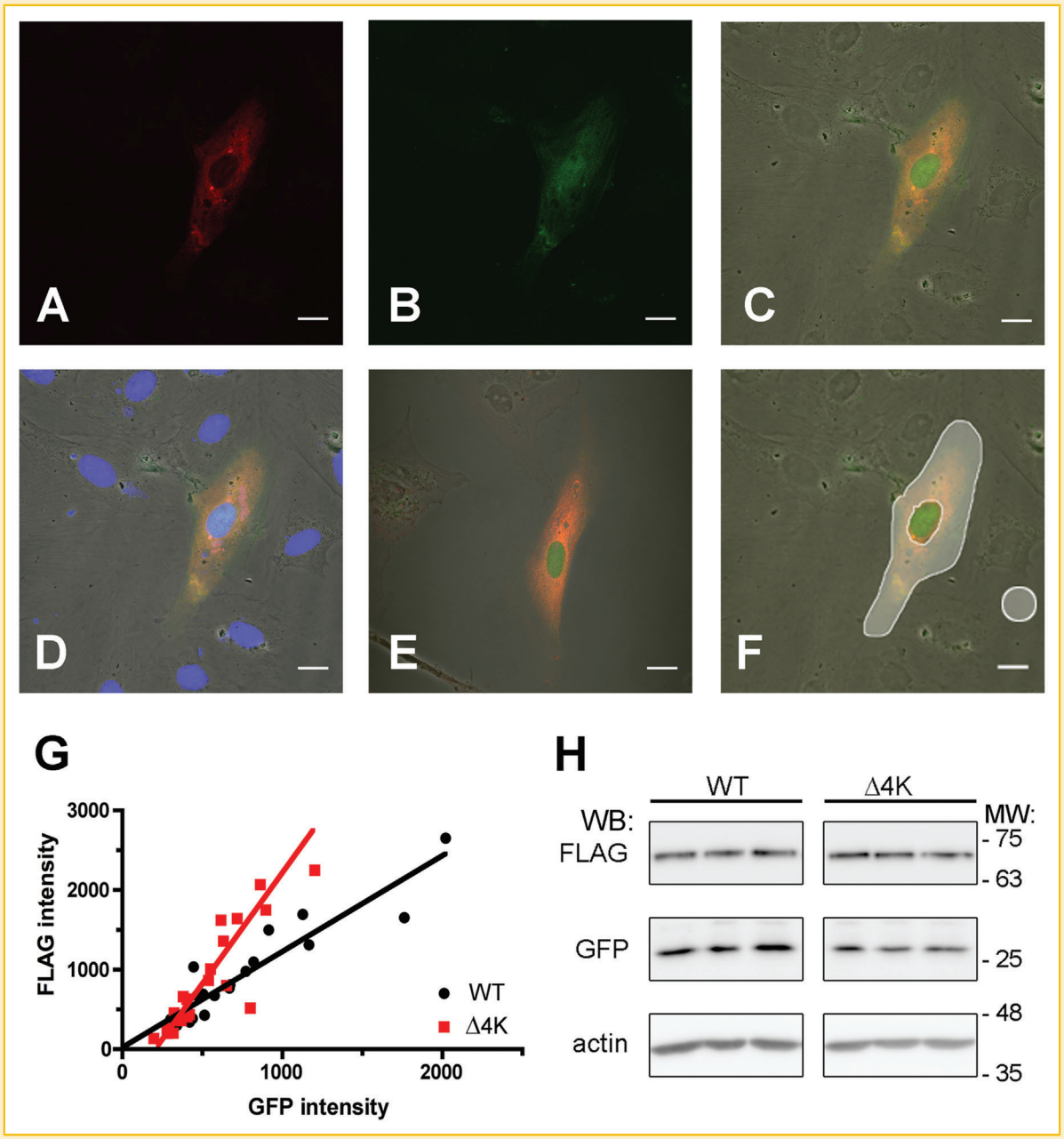

Fig. 3. The expression ratio relating the AcGFP signal to the FLAG-SMTNL1 fluctuates with the expression of different SMTNL1 protein variants. A7r5 cells were transfected with a bicistronic vector expressing FLAG-SMTNL1 (A–D,F) or FLAG-SMTNL1-Δ4K (E) together with AcGFP. Immunoreactivity towards the FLAG-tag was detected with mouse anti-FLAG M2 antibody and AlexaFluor 568 goat anti-mouse secondary antibody (red; λ_{ex} 559 nm, λ_{em} 570 ± 50 nm). In D, counter-stained nuclei are also shown (DAPI, blue; λ_{ex} 405 nm, λ_{em} 420 ± 20 nm). Fluorescence intensities for FLAG-SMTNL1 (A; red) and AcGFP (B; green) following immunocytochemistry were quantified. Phase contrast as shown in panels C–F was used to visualize non-transfected cells. In F, the region of interest (ROI) for measuring FLAG and AcGFP fluorescent intensities is highlighted in white. An extracellular area (circle) located in the bottom right was used for background subtraction. Scale bar: 20 μm. In G, the total cellular FLAG immunofluorescence and AcGFP intensities were quantified within the ROI using CellSens software (n = 21 cells, three independent experiments). FLAG-SMTNL1 (WT, black circles) or FLAG-SMTNL1−Δ4K (Δ4K, red squares) intensities were graphed versus AcGFP and linear regression calculated (black and red solid lines, respectively). In H, transfected cells were harvested from three independent experiments and FLAG-tagged protein, AcGFP and α-actin were detected by western blotting with the respective antibodies. Molecular weight (MW) markers in kDa are shown on the *right*.

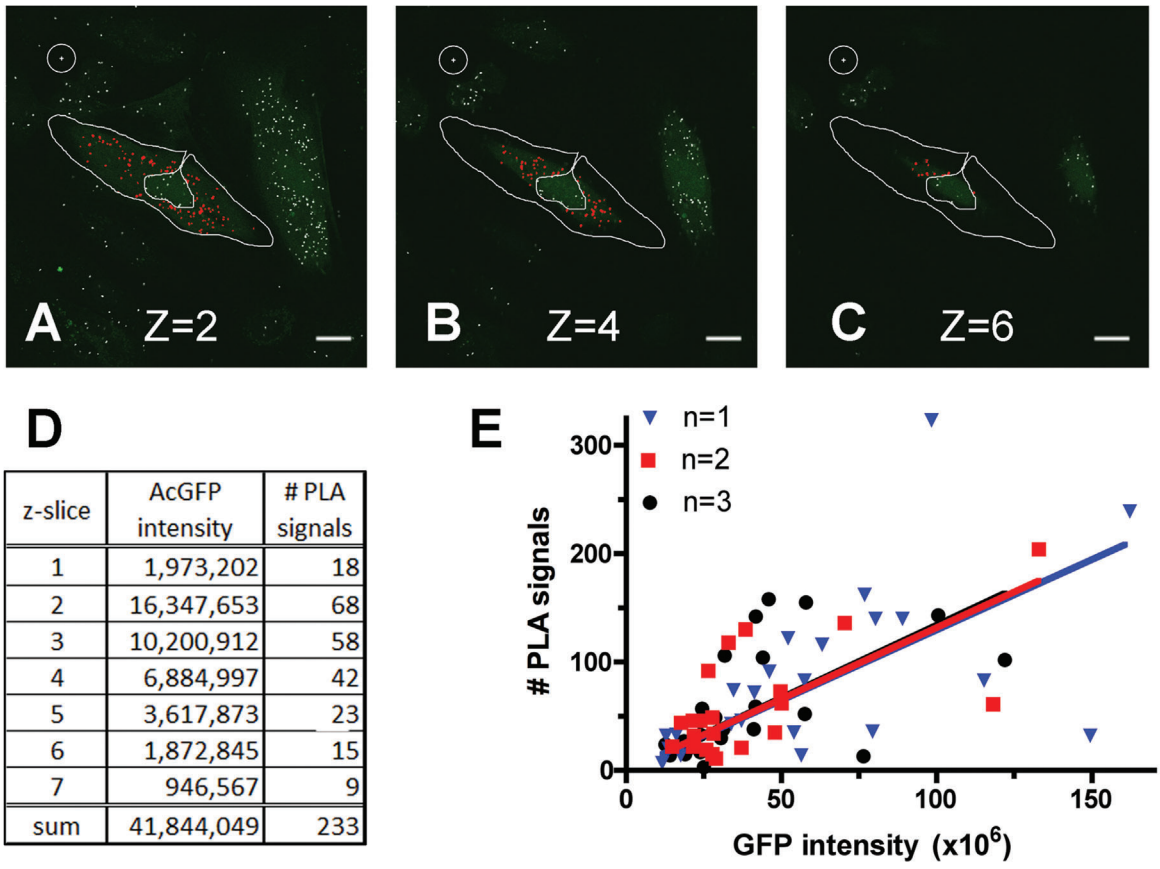

z-slice	AcGFP intensity	# PLA signals
1	1,973,202	18
2	16,347,653	68
3	10,200,912	58
4	6,884,997	42
5	3,617,873	23
6	1,872,845	15
7	946,567	9
sum	41,844,049	233

Fig. 4. SMTNL1–CaM proximity events can be quantified and expressed as a function of cellular SMTNL1 protein levels. The number of PLA signals is proportional to the AcGFP fluorescence intensity. A7r5 cells were transfected with a bicistronic vector expressing FLAG-SMTNL1 together with GFP (green) and probed with anti-FLAG and anti-CaM using the PLA kit. Transfected A7r5 cells were identified by green AcGFP fluorescence and red PLA signals. (A–C) Two regions of interest (ROIs) were selected: the cytoplasmic compartment (white cellular outline, excluding the nucleus) and the extracellular space for background correction (white circle, top left corner). The red channel was activated to display PLA signals (red dots). PLA signals within the intracellular ROI were counted (highlighted in red; signals not counted are in white) in all z-slices (thickness, $z = 1\ \mu m$). Examples of different z-slices are shown. Scale bar: 20 μm. In D, the integral of the calculated green (GFP) intensity and number of detected PLA signals in the ROI of each z-slice are tabulated. In E, the number of PLA signals was related to the AcGFP fluorescence intensity in the same ROI for individual cells of three independent experiments, each with ≥10 cells quantified from two slides each. To compare the independent experiments, the number of PLA signals and AcGFP intensity were normalized to [average AcGFP intensity] = 1.

quantification at the cellular level is difficult, and for the most part, PLA has been used to answer qualitative questions regarding protein associations [Edin et al., 2010; Gajadhar and Guha, 2010; Mocanu et al., 2011; Gajadhar et al., 2012; Jung et al., 2013]. To circumvent this issue, we developed a refinement of the PLA method to accurately quantify small changes in protein-protein proximity within transfected cells. We overcame the issue of differential protein expression by normalizing the PLA signal to protein expression levels within each cell using co-transfected AcGFP as a surrogate for SMTNL1 expression after transfection with a bicistronic vector delivering AcGFP and FLAG-SMTNL1. One important consequence of this refinement is the reduction in experimental error. Normalizing protein expression resulted in an error of ~10% after analyzing ~ 12 cells for each of $n = 3$ independent experiments. This is much improved over past reports; for example, an error of >17% was found for PLA measurements with quantification of 30 cells for $n = 3$ independent experiments where the transfection levels of target proteins were not assessed [Gajadhar and Guha, 2010].

In our studies, the relationship between AcGFP intensity and the number of PLA signals associated with CaM-SMTNL1 proximity remained linear even at high protein expression levels. The intensity of the AcGFP signals varied by 15-fold, and the PLA signal was not saturated within this range. Interestingly, when flow-cytometry was used to analyse PLA signals in a recent study, the number of PLA signals was not proportional to the protein expression [Mocanu et al., 2011]. In this case, the PLA signal reached a plateau at ~ 10-fold difference between the lowest and highest signal with moderate to high protein expression. The larger dynamic range observed in our study was likely due to inherent differences between flow-cytometry and immunocytochemistry as well as variations in optimizations for the PLA technique. We also found that our quantitative experiments

TABLE I. Relative Binding of SMTNL1 Mutants to CaM as Determined by In Situ PLA Analysis.

SMTNL1 Variant	% relative binding (PLA signal / FLAG intensity)*	*P* value[a]
WT	100 ± 6	
ΔCDB1	126 ± 16	n.s.[b]
scrCBD1	71 ± 9	$P < 0.05$
ΔCDB1−Δ4K	113 ± 16	n.s.
scrCDB1−Δ4K	74 ± 10	$P < 0.05$
Δ4K	117 ± 13	n.s.

AlexaFluor568 intensity (for FLAG), AcGFP intensity, and PLA signals were quantified and reported as the number of PLA signals per FLAG immunofluorescence intensity. The AcGFP fluorescence was used as a surrogate for FLAG-SMTNL1 expression in both PLA experiments and immunofluorescence imaging.

*Normalized to WT = 100% ± standard error of the mean.

[a]Compared to WT, by unpaired two-tailed Student's *t*-test with 95% confidence interval. n ≥21 cells from ≥4 slides per mutant.

[b]Not significantly different, (n.s.).

required optimization (i.e., antibody concentrations, incubation times and wash conditions) to avoid overlapping and touching PLA signals which might lead to an underestimate of CaM-SMTNL1 proximity events.

Our initial biochemical studies identified in vitro apo-CaM-binding properties for the IQ-motif (CBD2) of SMTNL1 [Ishida et al., 2008]. More recently, we have defined CBD1 of SMTNL1 as a canonical Ca-CaM-binding motif that binds Ca-CaM and weakly apo-CaM in vitro [Ulke-Lemee et al., 2014]. To assess the relevance of each CBD in situ, we mutated CBD1 and CBD2 in the SMTNL1 background and examined the importance of the two sites on SMTNL1-CaM proximity using PLA. The PLA data did not reveal any difference in CaM proximity upon mutation of CBD2 in unstimulated smooth muscle cells where $[Ca^{2+}]_i$ is estimated to be ~ 100 nM [Williams et al., 1985; Yagi et al., 1988; Campos-Toimil et al., 2005]. This was surprising because the Δ4K deletion (i.e., removal of terminal KTKKK sequence) eliminated apo-CaM-binding in vitro [Ulke-Lemee et al., 2014]. This could indicate that an additional CaM-binding site exists in the full-length SMTNL1 protein sequence or that the KTKKK residues are less important for CaM-binding than originally described for the isolated CH-domain [Ishida et al., 2008]. Alternatively, a third protein might mediate co-localization of SMTNL1 and CaM. Given the weak binding affinity of CBD2 to CaM in vitro and lack of effect of KTKKK deletion, it seems unlikely that this site contributes to CaM binding in situ.

It is thus expected that the measured in situ proximity of SMTNL1 to CaM is due to association with CBD1. We have previously observed that CBD1 has weak, but significant affinity for apo-CaM in vitro, and this affinity was reduced by mutation [Ulke-Lemee et al., 2014]. Indeed, scrambling the CBD1 sequence and replacing large hydrophobic amino acids significantly reduced in situ proximity to CaM. The complete deletion of CBD1 (i.e., ΔCDB1) did not affect proximity to apo-CaM as measured by PLA. This is a surprising result as we had established the importance of CBD1 in CaM proximity with the scrambled CBD1 variant. We have earlier reported that the intrinsically disordered domain of SMTNL1 can reduce affinity of CBD1 for apo-CaM and/or increase affinity for Ca-CaM [MacDonald et al., 2012; Ulke-Lemee et al., 2014]. It is possible that modification of this region by deleting CBD1 influenced intramolecular interactions between the CH domain and the intrinsically disordered region (IDR) and thus, resulted in higher apparent CaM-binding. Combining the scrambled CBD1 sequence with the truncation of CBD2 (i.e., SMTNL1-scrCBD1-Δ4K) did not further reduce in situ proximity. This is in contrast to in vitro pull-down studies where these mutations in CBD1 and CBD2 had an additive effect [Ulke-Lemee et al., 2014]. Taken together, the accumulated data suggest that SMTNL1 possesses two domains with CaM-binding affinity but only CBD1 provides binding to CaM in situ. This leaves the question as to why ~70% of proximity to apo-CaM is still observed in the smooth muscle cells when investigating the scrambled CBD1 with truncation of CBD2. First, CBD2 could contribute cooperatively to binding, and this was not reduced by the KTKKK deletion, as detailed above. Second, our earlier studies showed that additional CaM-binding site(s) in SMTNL1 seems to exist since CBD2 mutation did reduce, but not eliminate, CaM association in vitro [Ulke-Lemee et al., 2014]. However, bioinformatic analyses did not detect any additional CaM-binding sites, so any undefined CBDs in the SMTNL1 sequence would be of the non-canonical type. And lastly, since PLA measures proximity, not physical protein-protein interactions, it is possible that null-mutants (e.g., SMTNL1-scrCBD1-Δ4K) and CaM are located in close proximity within the cell, but without direct interaction.

ACKNOWLEDGMENTS

This work was supported by a research grant from the Canadian Institutes of Health Research (CIHR, MOP-97931). The authors thank Drs. Fiona Clement and Guanmin Chen (University of Calgary) for assistance with statistical assessments. A.U-L was recipient of a Heart & Stroke Foundation of Canada Fellowship. S.R.T. is recipient of a Alberta Innovates – Health Solutions (AIHS) Doctoral Scholarship and CIHR Canada Graduate Scholarship. J.A.M. is a recipient of an AIHS Senior Scholar award. The authors have no conflict of interest to declare.

REFERENCES

Bahler M,Rhoads A. 2002. Calmodulin signaling via the IQ motif. FEBS Lett 513:107–113.

Bodoor K, Lontay B, Safi R, Weitzel DH, Loiselle D, Wei Z, Lengyel S, McDonnell DP, Haystead TA. 2011. Smoothelin-like 1 protein is a bifunctional regulator of the progesterone receptor during pregnancy. J Biol Chem 286:31839–31851.

Borman MA, MacDonald JA, Haystead TA. 2004. Modulation of smooth muscle contractility by CHASM, a novel member of the smoothelin family of proteins. FEBS Lett 573:207–213.

Campos-Toimil M, Elies J, Orallo F. 2005. Trans- and cis-resveratrol increase cytoplasmic calcium levels in A7r5 vascular smooth muscle cells. Mol Nutr Food Res 49:396–404.

Chin D, Means AR. 2000. Calmodulin: A prototypical calcium sensor. Trends Cell Biol 10:322–328.

Edin S, Oruganti SR, Grundstrom C, Grundstrom T. 2010. Interaction of calmodulin with Bcl10 modulates NF-kappaB activation. Mol Immunol 47:2057–2064.

Gajadhar A, Guha A. 2010. A proximity ligation assay using transiently transfected, epitope-tagged proteins: Application for in situ detection of dimerized receptor tyrosine kinases. Biotechniques 48:145–152.

Gajadhar AS, Bogdanovic E, Munoz DM, Guha A. 2012. In situ analysis of mutant EGFRs prevalent in glioblastoma multiforme reveals aberrant dimerization, activation, and differential response to anti-EGFR targeted therapy. Mol Cancer Res 10:428–440.

Gimona M, Djinovic-Carugo K, Kranewitter WJ, Winder SJ. 2002. Functional plasticity of CH domains. FEBS Lett 513:98–106.

Ikura M. 2002. Calmodulin Target Database: Binding Site Search and Analysis. Available from http://calcium.uhnres.utoronto.ca/ctdb/ctdb/home.html.

Ishida H, Borman MA, Ostrander J, Vogel HJ, MacDonald JA. 2008. Solution structure of the calponin homology (CH) domain from the smoothelin-like 1 protein: A unique apocalmodulin-binding mode and the possible role of the C-terminal type-2 CH-domain in smooth muscle relaxation. J Biol Chem 283:20569–20578.

Ishida H, Vogel HJ. 2006. Protein-peptide interaction studies demonstrate the versatility of calmodulin target protein binding. Protein Pept Lett 13: 455–465.

Jung J, Lifland AW, Alonas EJ, Zurla C, Santangelo PJ. 2013. Characterization of mRNA-cytoskeleton interactions in situ using FMTRIP and proximity ligation. PLoS One 8:e74598.

Koos B, Andersson L, Clausson CM, Grannas K, Klaesson A, Cane G, Soderberg O. 2014. Analysis of protein interactions in situ by proximity ligation assays. Curr Top Microbiol Immunol 377:111–126.

Kramer J, Aguirre-Arteta AM, Thiel C, Gross CM, Dietz R, Cardoso MC, Leonhardt H. 1999. A novel isoform of the smooth muscle cell differentiation marker smoothelin. J Mol Med (Berl) 77:294–298.

Kramer J, Quensel C, Meding J, Cardoso MC, Leonhardt H. 2001. Identification and characterization of novel smoothelin isoforms in vascular smooth muscle. J Vasc Res 38:120–132.

Lontay B, Bodoor K, Weitzel DH, Loiselle D, Fortner C, Lengyel S, Zheng D, Devente J, Hickner R, Haystead TA. 2010. Smoothelin-like 1 protein regulates myosin phosphatase-targeting subunit 1 expression during sexual development and pregnancy. J Biol Chem 285:29357–29366.

MacDonald JA, Ishida H, Butler EI, Ulke-Lemee A, Chappellaz M, Tulk SE, Chik JK, Vogel HJ. 2012. Intrinsically disordered N-terminus of calponin homology-associated smooth muscle protein (CHASM) interacts with the calponin homology domain to enable tropomyosin binding. Biochemistry 51:2694–2705.

Mocanu MM, Varadi T, Szollosi J, Nagy P. 2011. Comparative analysis of fluorescence resonance energy transfer (FRET) and proximity ligation assay (PLA). Proteomics 11:2063–2070.

Niessen P, Clement S, Fontao L, Chaponnier C, Teunissen B, Rensen S, van Eys G, Gabbiani G. 2004. Biochemical evidence for interaction between smoothelin and filamentous actin. Exp Cell Res 292:170–178.

Niessen P, Rensen S, van Deursen J, De Man J, De Laet A, Vanderwinden JM, Wedel T, Baker D, Doevendans P, Hofker M, Gijbels M, van Eys G. 2005. Smoothelin-a is essential for functional intestinal smooth muscle contractility in mice. Gastroenterology 129:1592–1601.

O'Connell DJ, Bauer MC, O'Brien J, Johnson WM, Divizio CA, O'Kane SL, Berggard T, Merino A, Akerfeldt KS, Linse S, Cahill DJ. 2010. Integrated protein array screening and high throughput validation of 70 novel neural calmodulin-binding proteins. Mol Cell Proteomics 9:1118–1132.

Quensel C, Kramer J, Cardoso MC, Leonhardt H. 2002. Smoothelin contains a novel actin cytoskeleton localization sequence with similarity to troponin T. J Cell Biochem 85:403–409.

Soderberg O, Gullberg M, Jarvius M, Ridderstrale K, Leuchowius KJ, Jarvius J, Wester K, Hydbring P, Bahram F, Larsson LG, Landegren U. 2006. Direct observation of individual endogenous protein complexes in situ by proximity ligation. Nat Methods 3:995–1000.

Turner SR, MacDonald JA. 2014. Novel contributions of the smoothelin-like 1 protein in vascular smooth muscle contraction and its potential involvement in myogenic tone. Microcirculation 21:249–258.

Ulke-Lemee A, Ishida H, Borman MA, Valderrama A, Vogel HJ, MacDonald JA. 2010. Tropomyosin-binding properties of the CHASM protein are dependent upon its calponin homology domain. FEBS Lett 584:3311–3316.

Ulke-Lemee A, Ishida H, Chappellaz M, Vogel HJ, MacDonald JA. 2014. Two domains of the smoothelin-like 1 protein bind apo- and calcium-calmodulin independently. Biochim Biophys Acta 1844:1580–1590.

van der Loop FT, Schaart G, Timmer ED, Ramaekers FC, van Eys GJ. 1996. Smoothelin, a novel cytoskeletal protein specific for smooth muscle cells. J Cell Biol 134:401–411.

Wehrens XH, Mies B, Gimona M, Ramaekers FC, Van Eys GJ, Small JV. 1997. Localization of smoothelin in avian smooth muscle and identification of a vascular-specific isoform. FEBS Lett 405:315–320.

Williams DA, Fogarty KE, Tsien RY, Fay FS. 1985. Calcium gradients in single smooth muscle cells revealed by the digital imaging microscope using Fura-2. Nature 318:558–561.

Wooldridge AA, Fortner CN, Lontay B, Akimoto T, Neppl RL, Facemire C, Datto MB, Kwon A, McCook E, Li P, Wang S, Thresher RJ, Miller SE, Perriard JC, Gavin TP, Hickner RC, Coffman TM, Somlyo AV, Yan Z, Haystead TA. 2008. Deletion of the protein kinase A/protein kinase G target SMTNL1 promotes an exercise-adapted phenotype in vascular smooth muscle. J Biol Chem 283:11850–11859.

Yagi S, Becker PL, Fay FS. 1988. Relationship between force and Ca2+ concentration in smooth muscle as revealed by measurements on single cells. Proc Natl Acad Sci USA 85:4109–4113.

SUPPORTING INFORMATION

Additional supporting information may be found in the online version of this article at the publisher's web-site.